

## A Model of the Wave 1–Wave 2 Vacillation in the Winter Stratosphere

WALTER A. ROBINSON\*

*Department of Geological Sciences, Columbia University, New York, NY 10025 and NASA/Goddard Space Flight Center, Institute for Space Studies, New York, NY 10025*

(Manuscript received 22 February 1985, in final form 28 May 1985)

### ABSTRACT

A three-dimensional, severely truncated, quasi-geostrophic model in a beta channel is used to explore the dynamics of the observed anticorrelation between the amplitudes of planetary waves 1 and 2 in the Northern Hemisphere winter stratosphere. The model, which includes interactions among eight horizontal modes, generates realistic wave 1–wave 2 vacillations when westward traveling wave 1 interacts with stationary waves 1 and 2. It is found that while wave 1 oscillates in response to wave–mean flow interactions, the oscillations in the amplitude of wave 2 are driven primarily by wave–wave interactions. Experiments with a barotropic model reveal that the timing of the strongest wave–wave interactions is determined by the wave 1 interaction with the mean flow.

### 1. Introduction

The wintertime circulation of the stratosphere in high northern latitudes is dominated by one or two quasi-stationary waves on a strong westerly jet. The amplitudes and phases of these waves vary considerably with time, the largest variations occurring in association with stratospheric sudden warmings, minor warmings, or sudden coolings, events that involve rapid changes in both the waves and the zonally averaged circulation. But even when the stratosphere is relatively quiescent the waves are unsteady. Labitzki (1977) presented observations of the geopotential amplitudes of planetary waves 1 and 2 at 30 mb and 60°N for 12 winters. A conspicuous feature of these data is the tendency for the amplitudes of waves 1 and 2 to be anticorrelated on time scales ranging from longer than a month down to a week. Examination of her results for the 1975/76 winter reveals that the relationship between waves 1 and 2 was especially strong during this winter in which the zonally averaged circulation was unusually undisturbed.

Smith *et al.* (1984) studied the negative correlation between waves 1 and 2, denoted the wave 1–wave 2 vacillation, for the 1978/79 winter. During this winter the vacillation was clearly evident at 10 mb but was not apparent at 300 mb. The authors concluded that the wave 1–wave 2 vacillation was generated in the stratosphere. Their analysis of the potential enstrophy budgets of waves 1 and 2 showed wave–wave interactions to be as important as interactions with the mean

flow and generally more important than dissipation. While their results suggested that the wave 1–wave 2 vacillation originated in the stratosphere and involved wave–wave interactions, there was no obvious relationship between the sign and strength of the transfers of potential enstrophy between the waves and the behavior of the wave amplitudes.

There are at least three plausible mechanisms to explain the wave 1–wave 2 vacillation. McIntyre (1982) suggested that negative correlations between the strengths of waves 1 and 2 could result from variations in their tropospheric forcing. If the two waves are primarily forced by tropospheric geopotential anomalies in the North Atlantic and North Pacific Oceans, wave 1 will result when the anomalies have different signs, whereas anomalies with the same sign will generate wave 2. However, the absence of the vacillation at the tropopause, at least during the 1978/79 winter, argues against this idea.

Another possibility is that the amplitudes of the waves vary in response to changes in the zonal flow that cause the vertical propagation of one wave to be favored at the expense of the other. By this mechanism, the linear responses of the waves to a varying zonally averaged stratospheric circulation could cause a wave 1–wave 2 vacillation in the presence of constant tropospheric wave forcing. Quasi-periodic fluctuations in the strength of the polar night jet have been observed on time scales identical to those of the wave 1–wave 2 vacillation (van Loon *et al.*, 1975). However, the observations of Smith *et al.* suggested that the vacillation involves wave–wave interactions, and was not simply the passive response of the waves to changes in the mean flow.

\* Present affiliation: Department of Atmospheric Sciences, University of Washington, Seattle, WA 98195.

This paper is an investigation of a third possibility, consistent with the results of Smith *et al.*, that the wave 1-wave 2 vacillation comes about through direct non-linear interactions between the waves. Section 2 is a brief discussion of when wave-wave interactions are likely to be important in the stratosphere. It is found that wave-wave interactions arise from two distinct processes. Interactions can occur between steady waves with different zonal phase velocities or they can occur in association with wave-mean flow interactions induced by wave transience or dissipation. Section 3 describes a numerical model used to study the dynamics of wave-wave interactions in the stratosphere. The model is a severely truncated spectral representation of quasi-geostrophic dynamics in a beta channel. Section 4 reports results of model experiments in which a wave 1-wave 2 vacillation is produced by the interaction of westward traveling wave 1 with stationary waves 1 and 2. A barotropic version of the model is used to illuminate the mechanism by which the vacillations in waves 1 and 2 are synchronized, and these investigations are described in Section 5. Section 6 contains a summary of the results and a discussion of their relevance to the observed phenomenon.

## 2. Theory of wave-wave interactions

The dynamics of waves with planetary zonal scales, but which are confined to a narrow band of latitudes around the polar night jet, are well described by quasi-geostrophic dynamics on the beta-plane. The motion is governed by the conservation of quasi-geostrophic potential vorticity (PV) following geostrophic motion.

$$q_t + J(\Psi, q) = S \quad (1)$$

where  $\Psi$  is the geostrophic streamfunction,  $S$  is a source or sink of PV, and  $J(\ )$  is the horizontal Jacobian. The PV,  $q$ , is given by

$$q = \beta y + \nabla^2 \Psi + (\rho_0 \epsilon \Psi_z)_z / \rho_0, \quad (2)$$

where  $\beta$  is the meridional gradient of the vertical component of the planetary vorticity,  $\rho_0$  is the basic state density [ $\rho_0 = \exp(-z/H)$ , where  $H$  is the density scale height], and  $\epsilon$  is a stability parameter ( $\epsilon = f_0^2/N^2$ , where  $f_0$  is the Coriolis parameter and  $N$  is the Brunt-Väisälä frequency).

For the purpose of investigating interactions among waves  $\Psi$  and  $q$  are expanded in eigenfunctions of the horizontal Laplacian.

$$\Psi = \sum_n \Psi_n(z) f_n(x, y) \quad (3a)$$

$$q = \sum_n q_n(z) f_n(x, y), \quad (3b)$$

where  $\nabla^2 f_n = -K_n^2 f_n$ , and  $q_n = -K_n^2 \Psi_n + (\rho_0 \epsilon \Psi_{nz})_z / \rho_0$ . Here  $K_n^2$  is the squared magnitude of the horizontal

wavenumber of the  $n$ th mode. The three-dimensional analog to  $K_n^2$ , the effective square wavenumber,  $\alpha_n$ , can be defined:

$$\alpha_n = -q_n / \Psi_n = K_n^2 - (\rho_0 \epsilon \Psi_{nz})_z / (\rho_0 \Psi_n); \quad (4)$$

$\alpha_n$  is undefined if  $\Psi_n = 0$ .

If the dependence of  $S$  on  $q$  and  $\Psi$  is linear, then different waves are directly coupled only by the advection term in Eq. (1). The interaction between two modes (say  $n = 0$  and  $n = 1$ ) in terms of their effective square wavenumbers is given by

$$J(\Psi_0 f_0, q_1 f_1) + J(\Psi_1 f_1, q_0 f_0) \\ = J(f_0, f_1) \Psi_0 \Psi_1 (\alpha_0 - \alpha_1). \quad (5)$$

If  $\Psi_1 = 0$ , the interaction is simply  $J(f_0, f_1) \Psi_0 q_1$ . From Eq. (5) it is seen that for waves to interact they must have different effective square wavenumbers,  $\alpha_0 \neq \alpha_1$ , or one wave must satisfy  $\Psi_n = 0$ .

Some insight into how  $\alpha_n$  is determined may be gained by considering the linearized PV equation for a single wave propagating with zonal phase velocity,  $c$ , in a mean flow under the influence of dissipation (for simplicity treated as equal rates of Newtonian cooling and Rayleigh friction,  $\lambda$ ).

$$\lambda q' + ik(\bar{u} - c)q' + ik\bar{q}_y \Psi' = S'. \quad (6)$$

Here  $q'$  and  $\Psi'$  are the PV and streamfunction amplitudes of a wave with zonal wavenumber  $k$  and  $S'$  is a source of wave PV. The ratio of the wave PV to its streamfunction is

$$q' / \Psi' = -\{1 + i\lambda/[k(\bar{u} - c)]\} \{\bar{q}_y / (\bar{u} - c) \\ - iS' / [\Psi' k(\bar{u} - c)]\} \times \{1 + (\lambda/[k(\bar{u} - c)])^2\}^{-1}. \quad (7)$$

A single wave can be considered to comprise two orthogonal modes, separated in phase by one-quarter wavelength. In the absence of an external source of wave PV one mode is described by the real part of Eq. (7) which represents that portion of the wave PV that is in phase with the streamfunction. This mode has an effective square wavenumber given by

$$\alpha = \frac{\bar{q}_y}{(\bar{u} - c)} \{1 + (\lambda/[k(\bar{u} - c)])^2\}^{-1}. \quad (8)$$

The imaginary part of Eq. (7) corresponds to a mode with nonzero potential vorticity but with zero streamfunction. For a steady inviscid wave this second mode is absent, and for the remaining mode  $\alpha = \bar{q}_y / (\bar{u} - c)$ . For a stationary inviscid wave  $\alpha = \bar{q}_y / \bar{u}$ .

As has been pointed out by Derome (1984), if  $\bar{q}_y / \bar{u}$  depends only on  $z$ , then inviscid stationary waves, remote from their forcing, all have the same value of  $\alpha$  and do not interact. He showed observations of  $\bar{q}_y / \bar{u}$  in which this ratio is nearly constant in those regions of the winter stratosphere where the waves are strongest. For a linear wave, deviations from the stationary in-

viscid value of  $\alpha$  come about because of zonal propagation ( $c \neq 0$ ), or because of dissipation or transience ( $\lambda \neq 0$ ). That zonal propagation can induce wave-wave interactions is significant, because westward traveling wave 1 with a period of one to three weeks is often observed in middle to high northern latitudes (Madden, 1978). Westward wave 2 is also observed, but its stratospheric amplitude is much weaker (Walterscheid, 1980).

Dissipation and transience can lead to wave-wave interactions either through the modification of  $\alpha$  or by inducing a component of the wave PV which is in quadrature with its streamfunction. In Eqs. (7) and (8)  $\lambda$  can be considered a measure of the strength of wave transience or dissipation. From Eq. (8) it is seen that the deviation of  $\alpha$  from its steady inviscid value is quadratic in  $\lambda$  while the strength of the PV which is in quadrature with the streamfunction is linear in  $\lambda$ . Thus for weak transience or dissipation the latter effect should be more important in causing wave-wave interactions. The quadrature between this component of the wave PV and the streamfunction leads to a zonal mean transport of PV, so that the wave affects the mean flow. In violating wave-mean flow noninteraction conditions (Dickinson, 1969; Andrews and McIntyre, 1976; Boyd, 1976) dissipation and transience also cause wave-wave interactions.

### 3. Description of the model

Beta-channel models that include a single wave and its interaction with the mean flow have been used to study the dynamics of wave-mean flow interactions, particularly in the context of the stratospheric sudden warming (Geisler, 1974; Holton and Mass, 1976). Because the present hypothesis is that wave-wave interactions play an essential role in the wave 1-wave 2 vacillation, it is necessary to extend the standard quasi-linear model to include several horizontal modes. In the interest of simplicity the number of these modes is kept as small as will allow us to study the relevant dynamics. The present model has eight horizontal modes: two zonally symmetric modes and two meridional modes for each of three zonal wavenumbers. The streamfunction is given by

$$\Psi = \sum_{n=1}^2 \{ \Psi_n \cos(n\pi y/L) + \text{Re} \sum_{m=1}^3 \Psi_{mn} \exp(ikmx) \sin(n\pi y/L) \}. \quad (9)$$

Here  $L$  is the width of the channel, equivalent to a meridional extent of 40 degrees of latitude,  $y$  is the distance from the southern boundary, and  $k$  the gravest zonal wavenumber in the cyclic channel,  $k = (a \cos\theta)^{-1}$ , where  $\theta$  is the latitude at the center of the channel,

$60^\circ\text{N}$  and  $a$  is radius of the earth. The PV equation, Eq. (1), is solved at this truncation on 50 levels extending from the surface to 122.5 km. Dissipation is parameterized as Rayleigh friction and Newtonian cooling. The rates of Rayleigh damping are those used by Holton and Wehrbein (1980), and the Newtonian cooling rates are taken from Holton and Mass (1976). These profiles are shown in Fig. 1.

Dissipation moves the flow towards a zonally symmetric basic state which resembles a Northern Hemisphere January. This basic state is obtained by computing the meridional gradient of PV associated with the winds shown in Fig. 2a. To be consistent with the model truncation, both these winds and their associated gradient of PV are separately projected onto  $\sin(\pi y/L)$ . The resulting winds are shown in Fig. 2b. These are the winds that are used in the model integrations. The meridional gradients of PV obtained by this procedure are smaller and therefore more realistic than those that would have resulted if  $\bar{q}_y$  had been computed directly from the wind profile in Fig. 2b.

The appropriate boundary condition at the surface for Eq. (1) when a log-pressure vertical coordinate is used has been derived by Tung (1983). It can be written

$$\delta_t + J(\Psi, \delta) = -f_0(w_E + w_F) - D_N(\Psi_z - \Psi_{0z}), \quad z = 0 \quad (10a)$$

where

$$\delta = f_0 h + \epsilon(\Psi_z - N^2 \Psi/g), \quad z = 0. \quad (10b)$$

Here  $D_N$  is the rate of Newtonian cooling,  $\Psi_0$  is the streamfunction of the basic state toward which dissipation relaxes the flow,  $h$  is the height of topographic

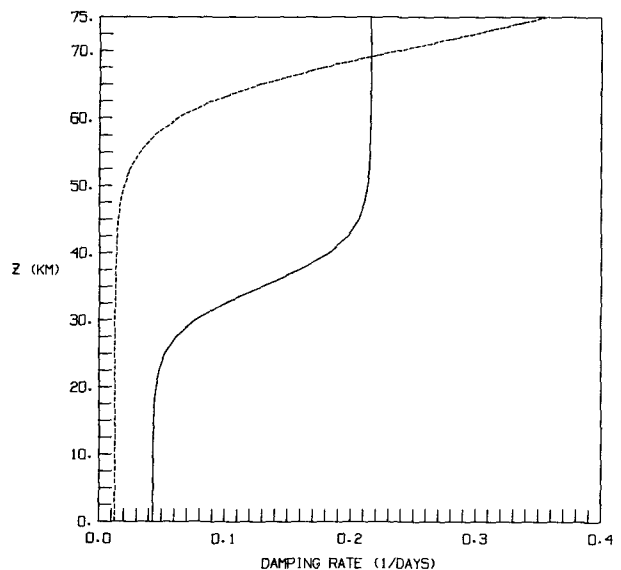


FIG. 1. Dissipation rates used in the model ( $\text{days}^{-1}$ ): Newtonian cooling (solid) and Rayleigh friction (dashed).

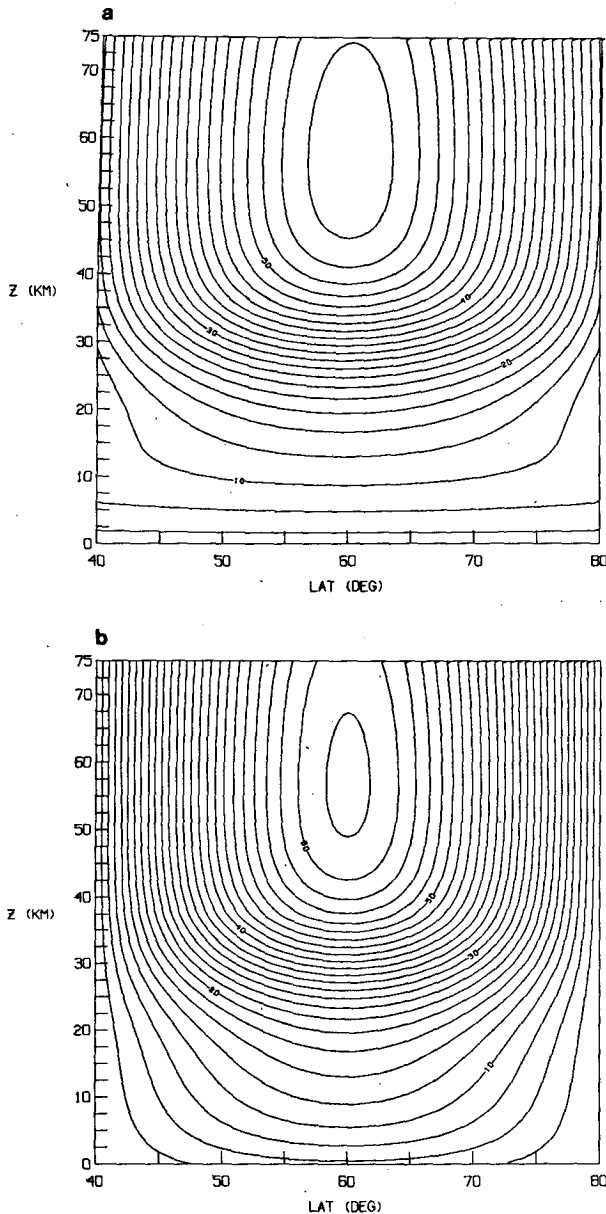


FIG. 2. Zonal wind profile ( $\text{m s}^{-1}$ ) for the zonally symmetric basic state used in the model. (a) Basic state used to compute the zonally symmetric potential vorticity; (b) projection of this state onto  $\sin(\pi y/L)$ .

relief, and  $g$  is the acceleration of gravity;  $w_E$  is the vertical velocity induced by Ekman suction at the top of the planetary boundary layer

$$w_E = D_E \nabla^2 (\Psi - \Psi_0), \quad z = 0 \quad (11)$$

where  $D_E$  is a depth equal to 150 m, and  $w_F$  is an imposed vertical velocity used to generate both stationary and traveling waves in the experiments described later.

For the vacillation experiments, we desire an initial state which includes a zonal flow and stationary waves in dynamic balance. In order to obtain such a state, the stationary waves are forced from the model's bottom boundary, and the model is integrated forward in time with the zonal flow fixed. The waves equilibrate to structures that are not the same as those of linear waves, because dissipation causes the waves to interact. (The interactions between stationary waves will be discussed in a paper in preparation.) Dissipation would also cause the waves to interact with the mean flow, tending to decelerate the westerlies. To compensate for this, a forcing is applied to the gravest zonally symmetric mode, which cancels the effect of the stationary waves, and this constant forcing is maintained throughout the time dependent experiments. The addition of this forcing is equivalent to strengthening the westerlies in the basic state toward which dissipation pushes the model. In the model this artifice represents the discrepancy in the atmosphere between the observed zonal winds and the winds that would occur in radiative equilibrium.

For the principal experiments described in the next section, initial conditions comprise the zonal wind profile shown in Fig. 2b, along with stationary waves 1 and 2, with amplitudes and phases shown in Fig. 3. (The phase is defined so as to be positive for a westward displacement of the wave.) The relative phases of the stationary waves are chosen so as to minimize their interactions in the stratosphere. Thus, the structures shown in Fig. 3 are nearly identical to those of linear waves. The initial conditions include other modes which are generated by the interaction of stationary waves 1 and 2, but these are very weak. The time evolution of the wave amplitudes in the vacillation experiments is not sensitive to the relative phases of the stationary waves, but the interpretation of the potential enstrophy budgets (see below) is simplified if nearly all the wave-wave interactions can be ascribed to the presence of a traveling wave.

The stationary initial state is disturbed by a westward traveling wave 1, which is generated by a westward moving distribution of vertical motion at the lower boundary. The traveling wave forcing is turned on slowly according to

$$w_F = W \exp(2i\pi t/T) \begin{cases} (1 - \cos(\pi t/\tau))/2, & t < \tau \\ 1, & t \geq \tau \end{cases} \quad (12)$$

where  $T$  is the period of the traveling forcing and  $\tau$  is a turn on time,  $\tau = 100$  days. For both stationary and traveling waves only the gravest meridional modes are forced from the boundary. This is consistent with the observed waves, which are typically weak in the tropics and show a single maximum in their amplitudes north of  $40^\circ\text{N}$  (van Loon *et al.*, 1973). The integration is

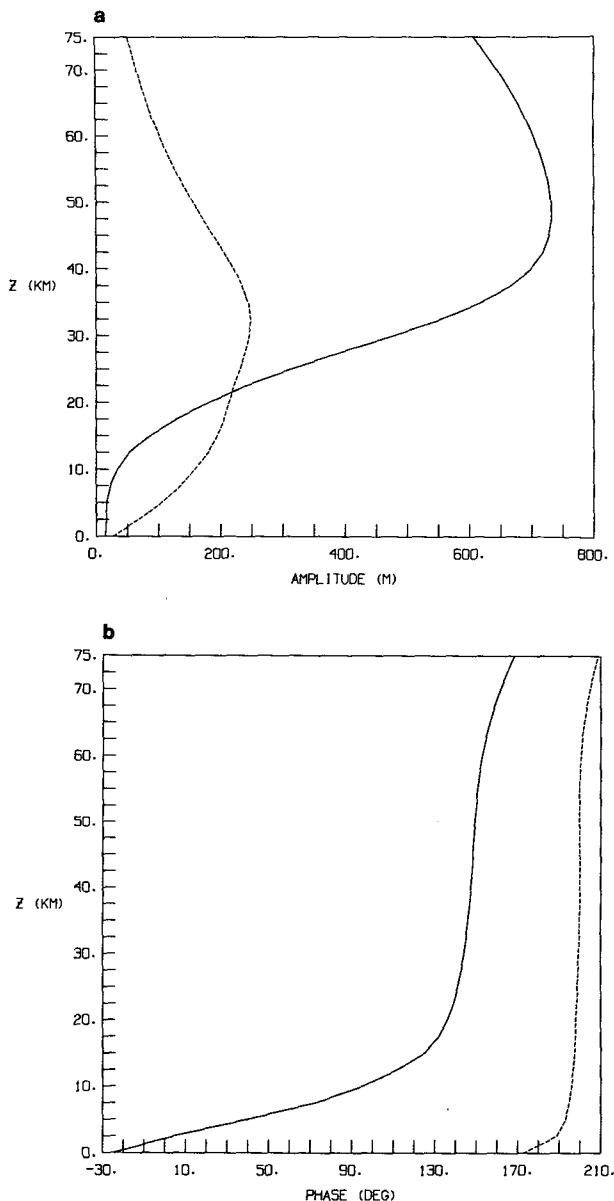


FIG. 3. Initial conditions for the (a) geopotential amplitude,  $m$ , and (b) phase (deg) of waves 1 (solid) and 2 (dashed) in model experiments.

continued until all transients have disappeared, and the model generates regular repeating vacillations. Traveling waves generated in this fashion are unrealistic in two respects. The observed amplitudes of traveling waves fluctuate on time scales similar to the periods of the waves (Lindzen *et al.*, 1984). However the quasi-periodic nature of the wave 1-wave 2 vacillation suggests that the essential physics will be retained when the vacillation is modeled as being truly periodic. Second, although observations of the vertical structures of traveling waves point to a tropospheric source, they

are presumably not generated at the surface. In what follows we will be concerned with wave-wave interactions in the stratosphere, so the conclusions will be unaffected by the nature and location of the tropospheric source of the westward wave.

#### 4. Results

For the first experiment (subsequently denoted the "standard vacillation") the initial state shown in Figs. 2b and 3 is disturbed by a westward traveling wave 1 forced by a vertical velocity of  $W = 0.001 \text{ m s}^{-1}$  with a period of 23.8 days. This is the period of the fastest westward free mode of wave 1 in the model when dissipation is excluded. This is a period longer than the 16 days characteristic of such waves in the atmosphere, a consequence of using a narrow channel. A wider channel would allow a better simulation of westward traveling waves, but the stationary waves are well reproduced in a channel 40 degrees wide, as was demonstrated by Simmons (1974). The amplitudes of westward wave 1 driven by a boundary forcing of  $0.001 \text{ m s}^{-1}$  at periods of 20, 23.8, and 30 days are shown in Fig. 4. (Reference to waves 1 and 2 denotes the gravest meridional modes of these waves. The higher meridional modes will be referred to as waves 1' and 2'.)

Figure 5 shows the vacillations in waves 1 and 2 and the mean flow at 32.5 km ( $\sim 10 \text{ mb}$ ) when westward wave 1 with a period of 23.8 days interacts with stationary waves 1 and 2 (Fig. 3). At this level the amplitude of the vacillation in wave 1 is about three times as large as the vacillation in wave 2. This ratio depends on the strength and the frequency of the wave forcing.

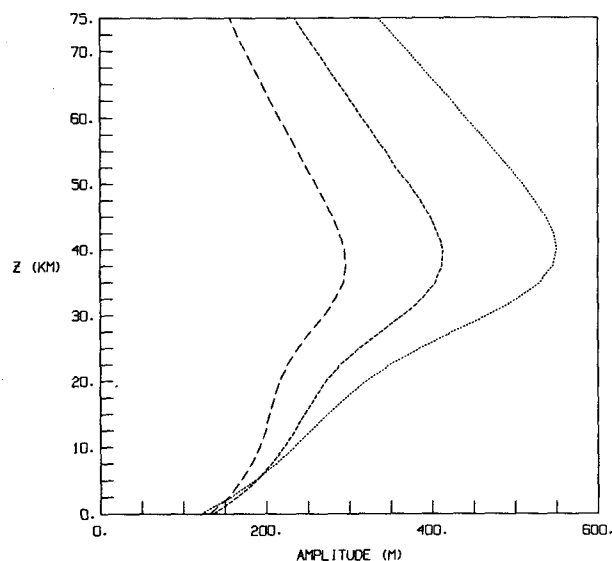


FIG. 4. Geopotential amplitude ( $m$ ) of westward traveling wave 1 at periods of 20 (long dashes), 23.8 (short dashes), and 30 (dots) days.

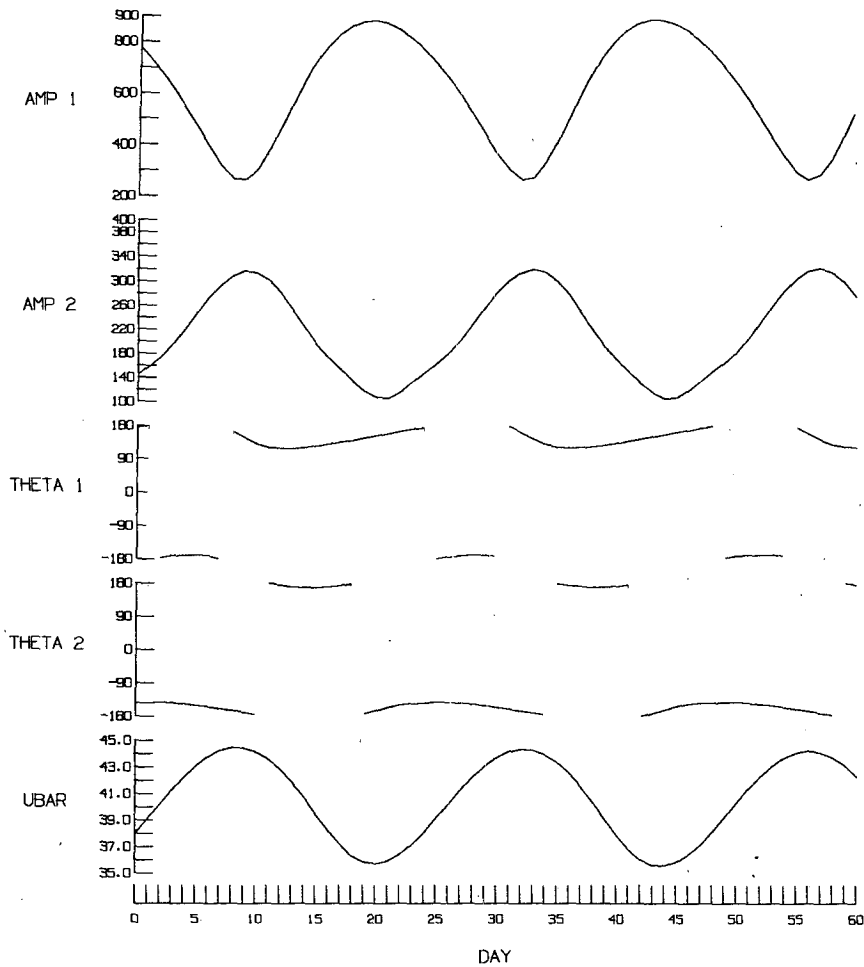


FIG. 5. Vacillations in the amplitudes ( $m$ ) and phases (deg) of waves 1 and 2 and the strength of the zonal jet ( $m\ s^{-1}$ ) at 10 mb, generated by the interaction of westward wave 1 (23.8 day period) with stationary waves 1 and 2 (see text). Phase is denoted "THETA".

The two vacillations are almost exactly 180 degrees out of phase. Despite the large changes in the wave amplitudes the zonal wind varies over less than  $10\ m\ s^{-1}$ . The vertical structure of this wave 1-wave 2 vacillation is shown in Figs. 6, 7, and 8 at times separated by six days, about one-quarter cycle. The strength of the zonal wind does not vary substantially in the troposphere, and the tropospheric vacillation in wave 1 is weaker than and out of phase with that in the stratosphere. This is consistent with the vacillation in the atmosphere. The anticorrelation of waves 1 and 2 is robust under changes in the frequency of the traveling wave, the amplitudes and relative phases of the stationary waves, and the strength of the zonal flow. For example, the vacillations generated by the interaction of the same stationary waves as before with westward wave 1 at traveling wave periods of 20 and 30 days are shown in Fig. 9a, b. While the strength of the wave 2 vacillation, relative to that of wave 1, decreases at the

longer period, the anticorrelation of the wave amplitudes is preserved. Further examples of the wave 1-wave 2 vacillation with altered stationary waves and in different zonal flows, which show the anticorrelation of the two waves, are shown in Robinson (1985).

Two distinct interactions contribute to the behavior displayed in these figures, the interaction of westward traveling wave 1 with stationary wave 2, and the interaction of the traveling wave with stationary wave 1. We consider their effects separately, beginning with the former. In the model the interaction of waves 1 and 2 acts primarily to force the second meridional mode of wave 1, denoted by wave 1'. This wave, with its small horizontal scale, is trapped near the altitude at which it is generated. Because this wave is responsible for the interaction of waves 1 and 2, these interactions tend to be much more local in altitude than the long waves themselves. Wave 1' is generated at the expense of stationary wave 2, as is seen in Fig. 10, which shows the

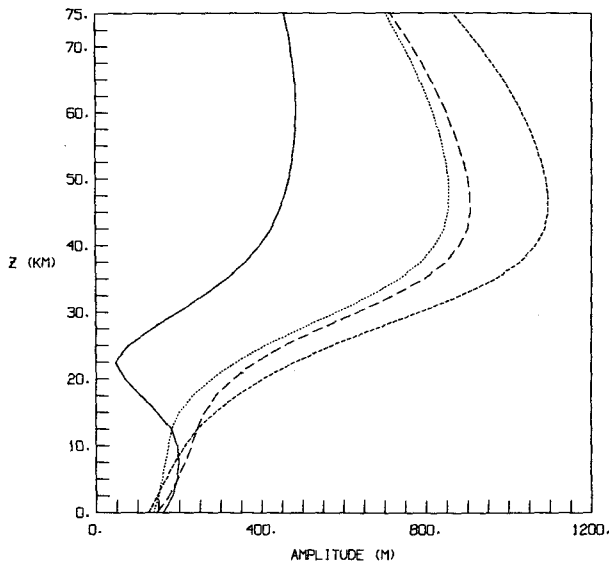


FIG. 6. Amplitude ( $m$ ) of wave 1 at day 0 (solid), 6 (long dashes), 12 (short dashes), and 18 (dots) of vacillation shown in Fig. 5.

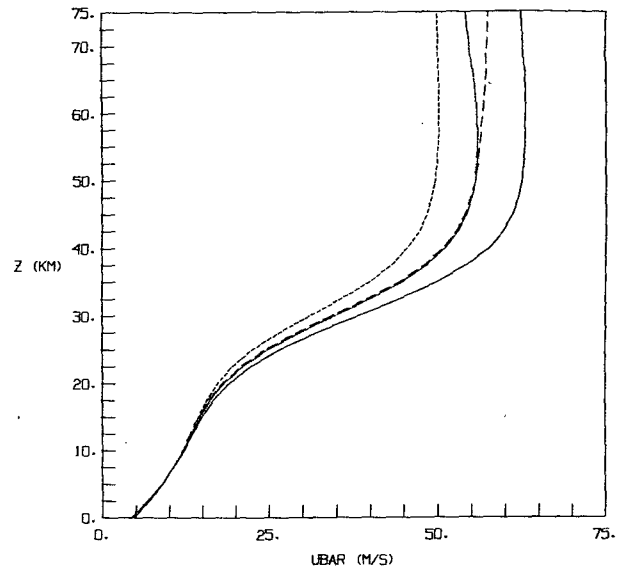


FIG. 8. As in Fig. 6 but for strength of the zonal jet ( $m s^{-1}$ ).

structure of stationary wave 2 when it interacts with westward wave 1, forced at periods of 20, 23.8, and 30 days with a vertical velocity of  $0.001 m s^{-1}$ . The interaction with wave 1 acts to dissipate wave 2 in the stratosphere, decreasing its amplitude and increasing its westward slope with height. Because the strength of this interaction is independent of the relative phases of the waves, this is a steady picture. This interaction causes no vacillations either in the wave amplitudes or in the mean flow.

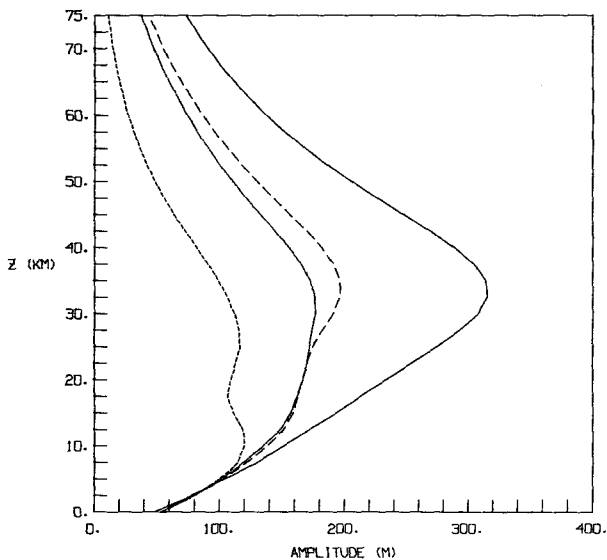


FIG. 7. As in Fig. 6 but for wave 2.

Waves 3 and 3' are also generated by wave-wave interactions during the vacillation, but they are relatively weak. The results change only slightly when the model is truncated at zonal wavenumber 2. The presence or absence of waves 3 and 3' does not affect the negative correlation between the amplitudes of waves 1 and 2.

The interference of the westward traveling and stationary components of wave 1 causes a vacillation in both the amplitude of the wave and the strength of the zonal flow. The theory of such interference-generated vacillations was discussed by Lindzen *et al.* (1982), and Madden (1983) described observations of this effect in the winter stratosphere. The evolution of vacillations generated by the interference of westward and stationary wave 1 in the model is shown in Fig. 11, for the 10 mb level. The traveling waves shown in Fig. 4 are forced in the presence of stationary wave 1 (shown in Fig. 3). At this level, remote from any wave forcing, wave 1 grows and decays by exchanging energy with the mean flow. Thus the minima in the zonal wind coincide with the maximum amplitudes of wave 1. The amplitude and phase of wave 1 trace distorted sinusoids. As discussed by Lindzen *et al.*, this is a consequence of the linear interference of the stationary and traveling components of the wave, and does not depend on the induced vacillation in the mean flow.

These results show that traveling wave 1 interacts strongly with stationary wave 2, and that the interference of westward and stationary wave 1 leads to vacillations in wave 1 and in the zonal wind. It seems plausible that the variation in the amplitude of wave 1, brought on by the interference of the stationary and traveling waves, could modulate the strength of the

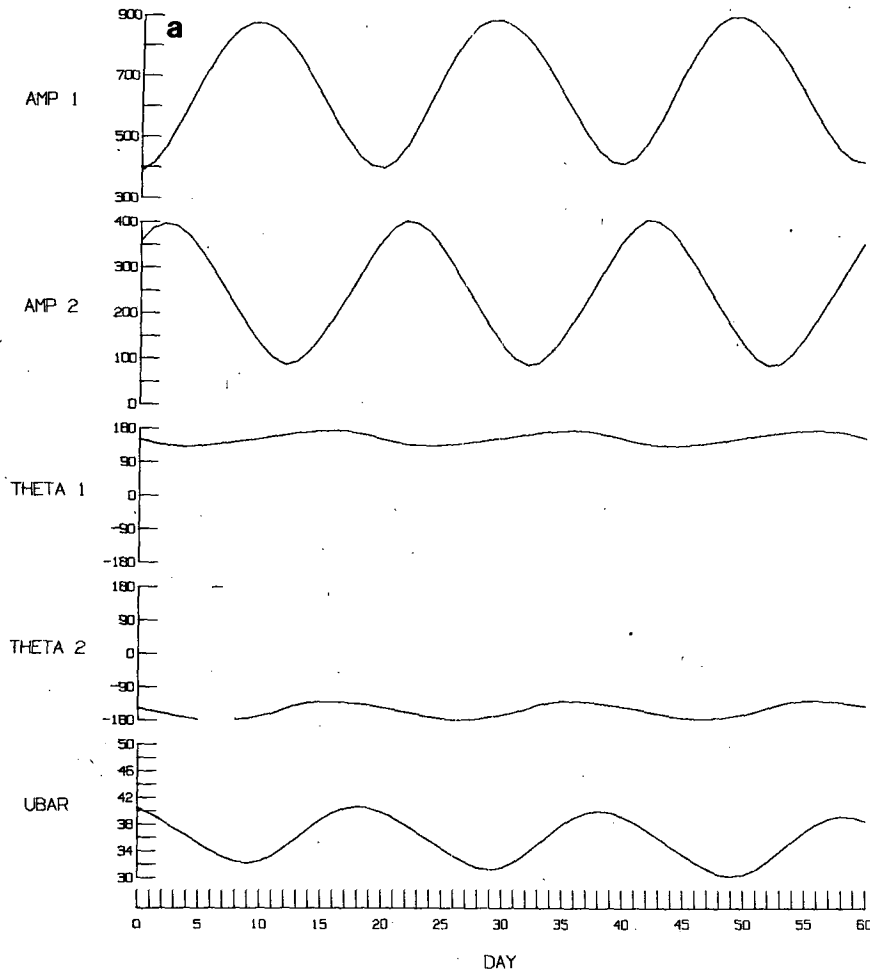


FIG. 9. As in Fig. 5 but for westward traveling wave 1 periods of (a) 20 and (b) 30 days.

nonlinear interaction between waves 1 and 2, inducing the vacillation in the latter wave seen in Fig. 5. However, it is not clear how the relative phases of the vacillations in the two waves are selected.

In order to understand the mechanics of the vacillation, it proves useful to consider the potential enstrophy (PE) budgets of the waves. Potential enstrophy is a useful diagnostic quantity because, like the wave energy, it is a positive measure of the strength of a wave, but unlike the energy, it is separately conserved at every level of the atmosphere (in the quasi-geostrophic system). The PE equation is obtained by multiplying Eq. (1) by  $q$ , giving

$$Q_t + J(\Psi, Q) = qS \quad (13a)$$

where

$$Q = q^2/2. \quad (13b)$$

Following Smith (1983), by multiplying the PV equa-

tion for each mode by the PV of that mode, Eq. (13) can be written in spectral form. For each wave

$$Q_t = Q_{MF} + Q_{WW} + Q_D, \quad (14)$$

where  $Q_{MF}$  is the rate at which the wave extracts PE from the zonal flow,  $Q_{WW}$  is the rate at which the wave gains PE from wave-wave interactions, and  $Q_D$  is the rate at which PE is lost to dissipation. The PE budget for a wave allows the importance of the different dynamic processes, wave-mean flow interactions, wave-wave interactions, and dissipation, to be compared.

Figure 12 shows the PE budget for wave 1 at 10 mb for the standard vacillation. The change of wave 1 PE with time is largely determined by the interaction of wave 1 with the mean flow. Dissipation causes a slight displacement of  $Q_t$  from  $Q_{MF}$ , and  $Q_{WW}$  is relatively unimportant. This suggests that wave-wave interactions have little effect on the wave 1 dynamics, so that with or without wave 2 present the vacillation of wave

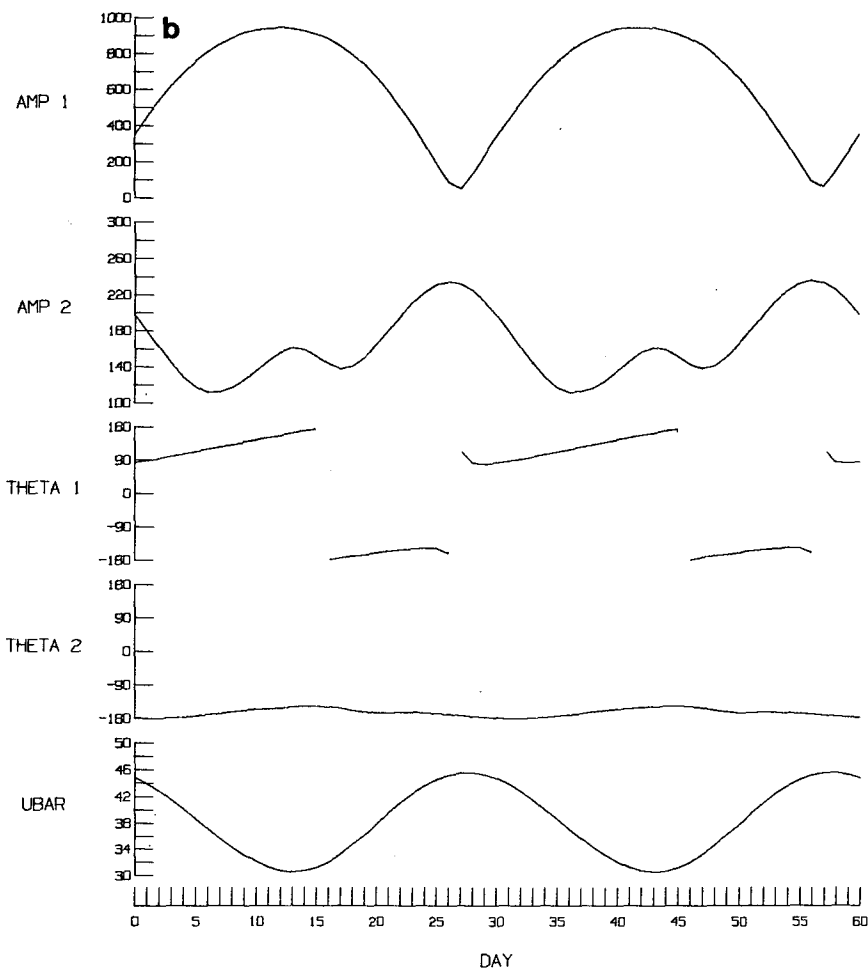


FIG. 9. (Continued)

1 is driven by the simple interference of its stationary and traveling components. This is confirmed by comparing Fig. 12 with Fig. 13, which shows the PE budget for the wave 1 interference vacillation (short dashes in Fig. 11) for which wave 2 is entirely absent. Figures 12 and 13 are very similar (note the change in scale), though of course  $Q_{WW} = 0$  in Fig. 13. The PE budget for wave 1 is dominated by  $Q_{MF}$  in all the model experiments. This term shows a nearly sinusoidal evolution in time, leading the amplitude of wave 1 by one-quarter of a vacillation period.

Having established that wave-wave interactions are unimportant for the wave 1 vacillation, we turn our attention to wave 2. Figure 14 shows the PE budget for wave 2 at 10 mb during the standard vacillation. Its behavior is more complicated than that for wave 1, with wave-mean flow and wave-wave interactions playing roles of equal importance. Averaged over time  $Q_{WW}$  is negative and  $Q_{MF}$  is positive. This is consistent

with the results for the interaction between stationary wave 2 and westward wave 1 (Fig. 10), which showed that this interaction tended to dissipate wave 2. However it is the time dependence of these interactions that is important in the vacillation. The rate  $Q_{WW}$  oscillates both with the same period and one-half the period of the westward wave 1;  $Q_{WW}$  is most negative when  $Q_{MF}$  for wave 1 is a maximum. Comparison with Fig. 12 indicates that most of the lost wave 2 PE is gained by wave 1. This pulse in the rate at which wave 2 loses PE to wave-wave interactions, coinciding with the most rapid growth of wave 1, is a feature common to all the cases of the wave 1-wave 2 vacillation generated by the model. Figure 15a, b shows the PE budgets for wave 2 at 10 mb for the 20- and 30-day vacillations (Fig. 9a, b). In both cases there is a negative pulse in  $Q_{WW}$ , which coincides with the fastest growth of wave 1: days 7, 27, and 47 in Fig. 15a, and days 1 and 31 in Fig. 15b. For the 30-day vacillation this correspondence

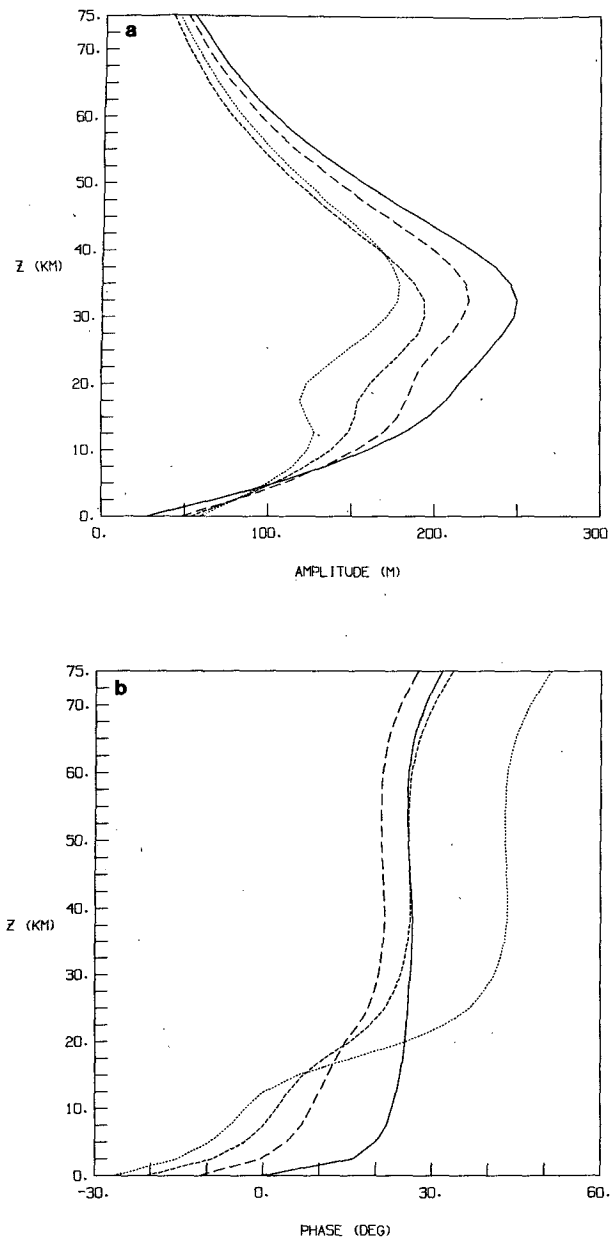


FIG. 10. (a) Amplitude,  $m$ , and (b) phase (deg) of stationary wave 2 modified by its interaction with westward wave 1 with periods of 20 (long dashes), 23.8 (short dashes), and 30 days (dots). The solid curves show the structure of wave 2 when wave 1 is absent.

still holds, even though the most negative values of  $Q_{WW}$  occur on days 15 and 45, during the declining phase of wave 1. This pulse of PE transfer out of wave 2 appears to play a crucial role in aligning the maxima of wave 1 with the minima of wave 2, i.e., in producing in the model the observed negative correlation between the amplitudes of the two waves.

## 5. Barotropic experiments

In the three-dimensional model the anticorrelation of waves 1 and 2, and thus the resemblance of the model's behavior to that of the atmosphere, depends on a strong transfer of PE from wave 2 to wave 1 during the increasing phase of the latter wave. Understanding which mechanism determines the timing of this transfer is difficult. The interference of the stationary and traveling components of wave 1 causes several quantities to vacillate simultaneously, the amplitude and phase of wave 1, the zonal wind speed, and the strength of wave 1's interaction with the mean flow, and it is not clear which is responsible for the variations in the non-linear forcing of wave 2. In order to isolate the effects of the oscillations in these quantities on the wave 1-wave 2 interaction, a barotropic model was constructed. This model exploits the nearly equivalent barotropic nature of the three waves responsible for the wave 1-wave 2 vacillation in the three dimensional model, stationary waves 1 and 2 and westward wave 1. The model describes the quasi-geostrophic motion of a barotropic fluid confined between rigid upper and lower boundaries in a beta-channel. Eq. (1) is still the appropriate PV equation for the motion, but now  $q$  is given by

$$q = \beta y + \nabla^2 \Psi + f_0 h / H. \quad (15)$$

$H$  is the average depth of the fluid and  $h$  is the amplitude of bottom relief, so that the depth is given by  $H - h$ . The source term [ $S$  in Eq. (1)] includes both imposed wave forcing and the damping of the motion towards a zonally symmetric basic state

$$S = D \nabla^2 (\Psi_0 - \Psi) + F \quad (16)$$

where  $D$  is a damping rate ( $D = 10^{-6} \text{ s}^{-1}$ ), and  $\Psi_0$  is the streamfunction of a zonally symmetric basic state

$$\Psi_0 = UL \cos(\pi y / L) / \pi, \quad (17)$$

where  $U$ , the velocity of the zonal wind at the center of the channel is taken equal to  $40 \text{ m s}^{-1}$ .

Waves can arise either from bottom relief or from imposed forcing [ $F$  in Eq. (15)]. In the latter case the PV of the  $n$ th mode is given by  $q_n = -K_n^2 \Psi_n$ . There can be no quadrature between the wave's streamfunction and its PV, and therefore no interaction between a single wave and the mean flow is allowed. By comparing results from experiments in which wave 1 is forced by bottom relief or by  $F$ , the importance of the interaction between wave 1 and the mean flow in the wave 1-wave 2 interaction can be determined.

The two-dimensional experiments follow the paradigm described in Section 4. Initial conditions consist of stationary waves 1 and 2 in equilibrium with the zonal flow. Westward traveling wave 1 is driven at its free wave period (15 days for this mean flow and channel width) by forcing that is turned on according to

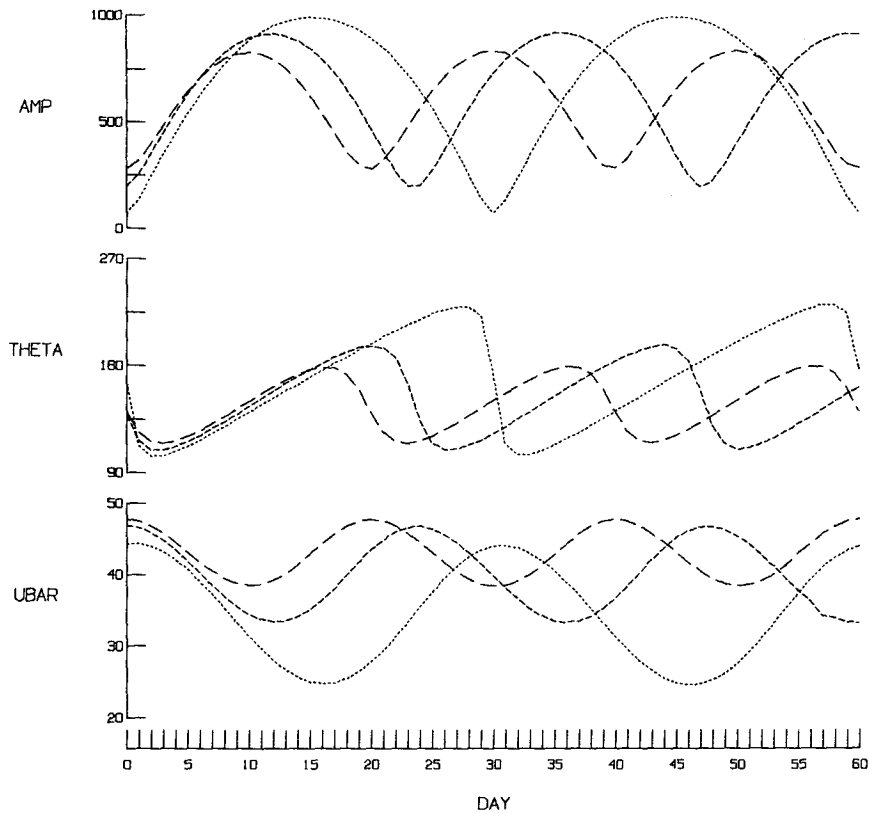


FIG. 11. Vacillations in the amplitude ( $m$ ) and phase (deg) of wave 1 and the strength of the zonal jet ( $m\ s^{-1}$ ) at 10 mb generated by the interference of stationary wave 1 and westward wave 1 with periods of 20 (long dashes), 23.8 (short dashes), and 30 days (dots).

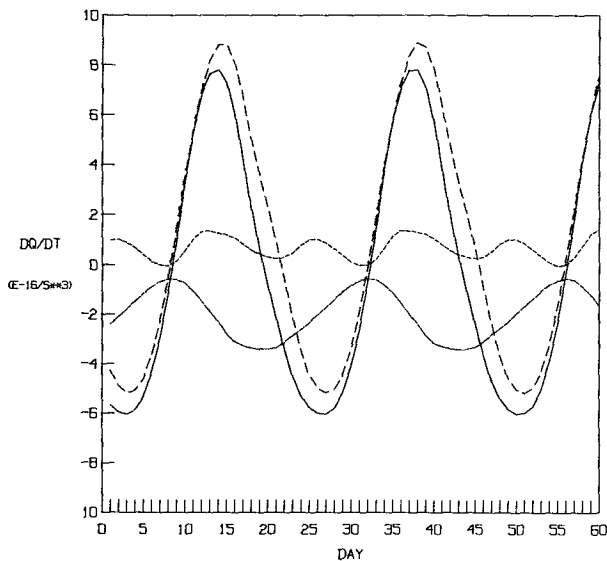


FIG. 12. Potential enstrophy budget for wave 1 at 10 mb in standard vacillation: rate of change of PE (solid), rate of gain of PE from the mean flow (long dashes), rate of gain of PE from wave-wave interactions (short dashes), rate of gain of PE from dissipation (dots). Units are  $10^{-16}\ s^{-3}$ .

Eq. (12). The forcing, whether or not it is due to bottom relief, can be defined by an amplitude of bottom relief,

$$F = -f_0(\bar{u}h_x + h_t)/H. \quad (18)$$

The values given correspond to a value of 7 km for  $H$ , the mean depth of the fluid.

Results of two-dimensional experiments will be most clearly analogous to the three-dimensional results when waves 1 and 2 are both forced by bottom relief, and are therefore able to interact with the zonal flow. When stationary waves 1 and 2 are forced so as to achieve amplitudes of 500 and 250 m respectively, and westward wave 1 is driven by bottom relief of 50 m with a period of 15 days, the resulting wave 1-wave 2 vacillation (Fig. 16) shares several features with the vacillation in the three-dimensional model. Both the amplitude of wave 2 and the strength of the zonal jet vary in opposition to the amplitude of wave 1, and the magnitude of the oscillation in the amplitude of wave 2 is smaller than that for wave 1. The PE budgets for this vacillation (Fig. 17a, b) also resemble the three-dimensional results. The PE of wave 1 varies in response to its interaction with the mean flow, while the wave 2

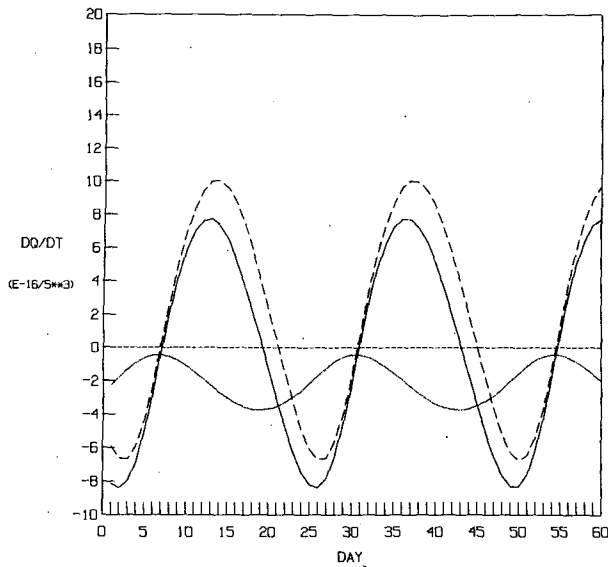


FIG. 13. As in Fig. 12 but for vacillation with wave 2 absent.

vacillation is driven by wave-wave interactions. Wave 2 loses PE to wave 1 most rapidly on days 10, 25, 40, and 55, when  $Q_{MF}$  for wave 1 is largest.

This experiment is repeated with the same parameters, with the PV of both the stationary and traveling components of wave 1 forced at the same rate as before but by external forcing as opposed to bottom relief. Wave 1 is thus unable to interact with the zonal flow. The evolution of this vacillation, shown in Fig. 18, indicates that changing the nature of the wave 1 forcing

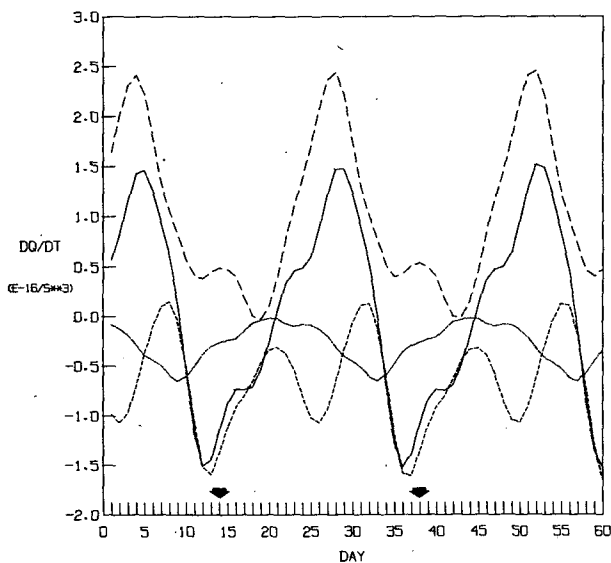


FIG. 14. As in Fig. 12 but for wave 2. The arrows show the times of the maxima in  $Q_{MF}$  for wave 1.

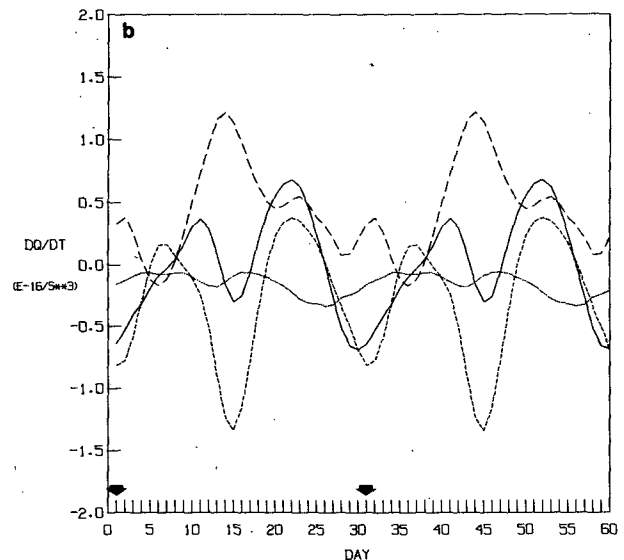
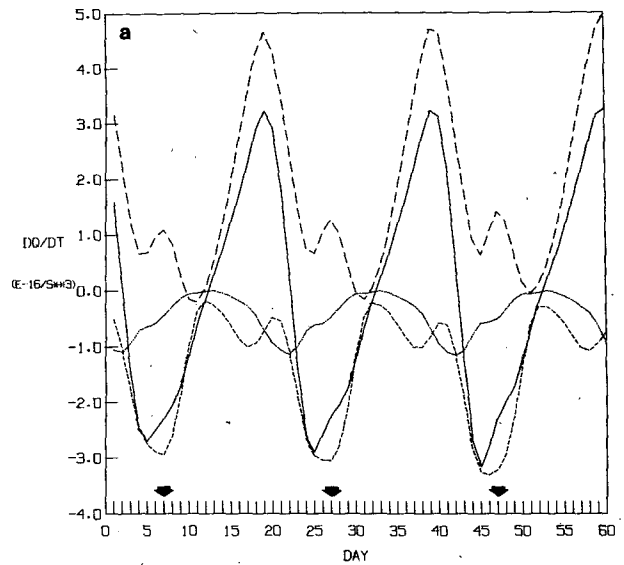


FIG. 15. As in Fig. 14 but for vacillations with periods of (a) 20 and (b) 30 days.

alters the behavior dramatically. The oscillations in waves 1 and 2 are now in phase, and the variations in the zonal wind are much weaker than in the previous experiment. The latter result is expected, as the large oscillations in the previous two-dimensional as well as the three-dimensional experiments resulted from the wave 1 interaction with the mean flow. The extraction of PE by wave-wave interactions still dominates the evolution of the wave 2 PE, but in the absence of wave 1-mean flow interactions the peaks in this term are no longer locked to the growing phase of wave 1.

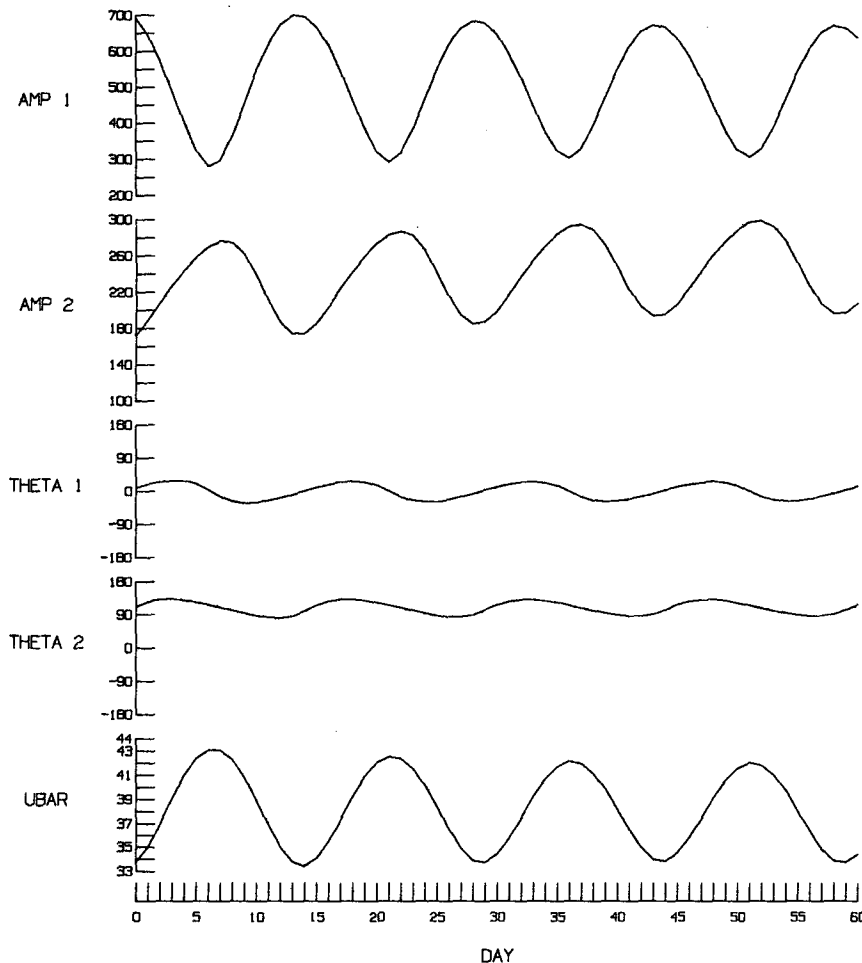


FIG. 16. As in Fig. 5 but for barotropic vacillation at period of 15 days.

This vacillation does not show the inverse relationship between waves 1 and 2 that is seen in the three-dimensional model and the atmosphere, and it differs from the previous barotropic experiment in its lack of wave 1–mean flow interaction and in the absence of a strong oscillation in the zonal wind. In order to determine which of these factors is responsible for the anticorrelation of waves 1 and 2, the experiment is repeated a second time using bottom relief to force wave 1, but holding the zonal wind fixed at  $40 \text{ m s}^{-1}$ . While this experiment is unphysical in that PV and PE are not conserved, it is useful for determining the role of the mean flow vacillation. Figure 19 shows the results of this experiment. In its details the vacillation is different from that shown in Fig. 16, but the inverse relationship between waves 1 and 2 is preserved, and the time dependence of the PE budget for wave 2 (not shown) is still dominated by  $Q_{WW}$ . We conclude that the wave–wave interactions which drive the wave 1–wave 2 vacillation results from the interaction of wave

1 with the mean flow, and that variations in the zonal wind do not play an essential role in the wave 1–wave 2 vacillation. This general conclusion, that the vacillation in the barotropic model only shows the observed phase lag between the oscillations in waves 1 and 2 when wave 1 is permitted to interact with the zonal flow, holds over a wide range of parameters, and shows little sensitivity to changes in the zonal flow, the period of the forcing, or the amplitudes of the waves. In addition, experiments in which the strength of the zonal wind is varied by external forcing fail to show the characteristic wave 1–wave 2 vacillation.

## 6. Summary and conclusion

We have seen that realistic wave 1–wave 2 vacillations are generated in a severely truncated, quasi-geostrophic model by the interaction of westward traveling wave 1 with stationary waves 1 and 2. Vacillations in wave 1 and the mean flow result from interference be-

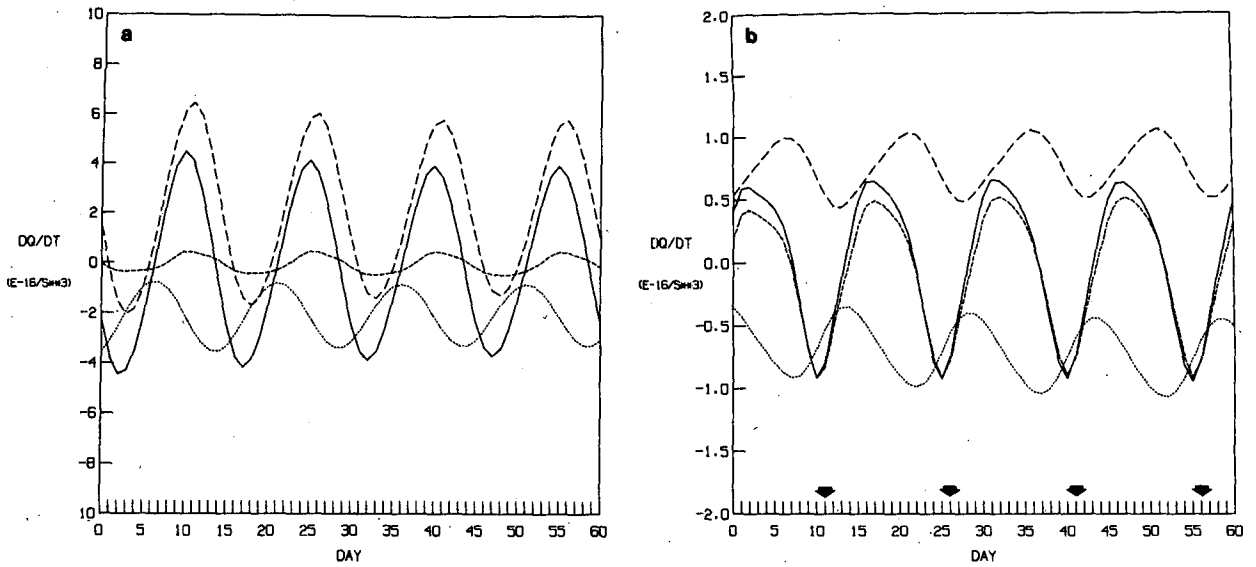


FIG. 17. PE budgets for (a) wave 1 and (b) wave 2 in barotropic vacillation shown in Fig. 16.

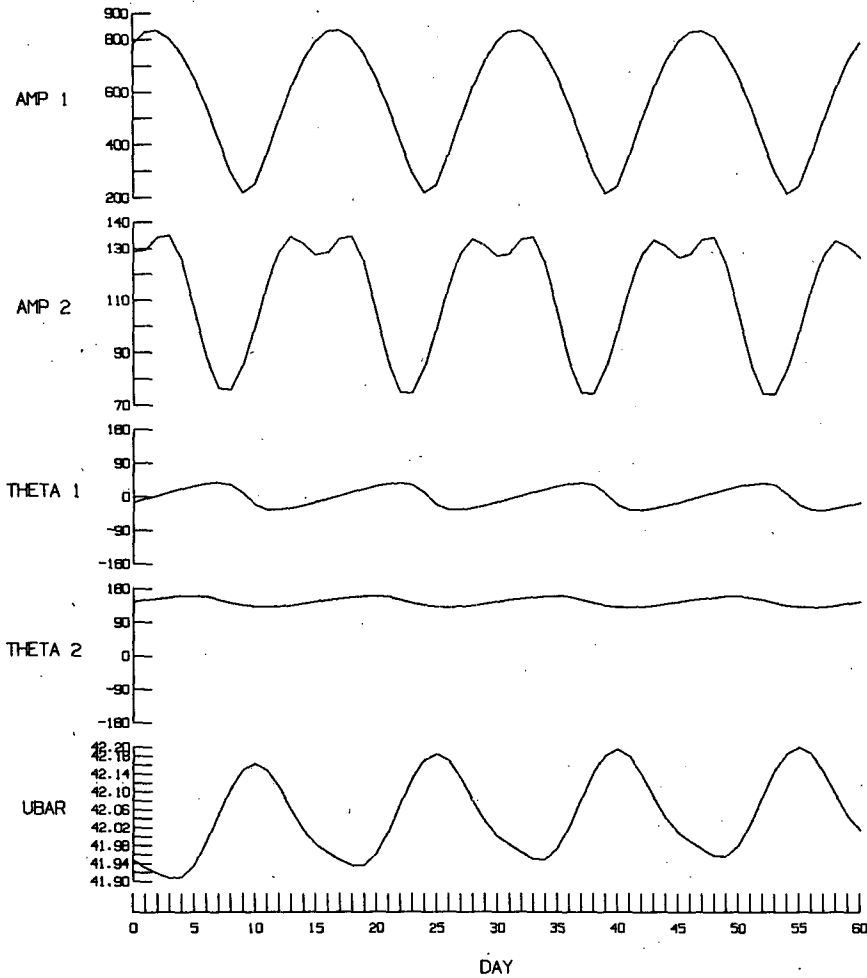


FIG. 18. As in Fig. 16 but for vacillation with wave 1 forced nontopographically.

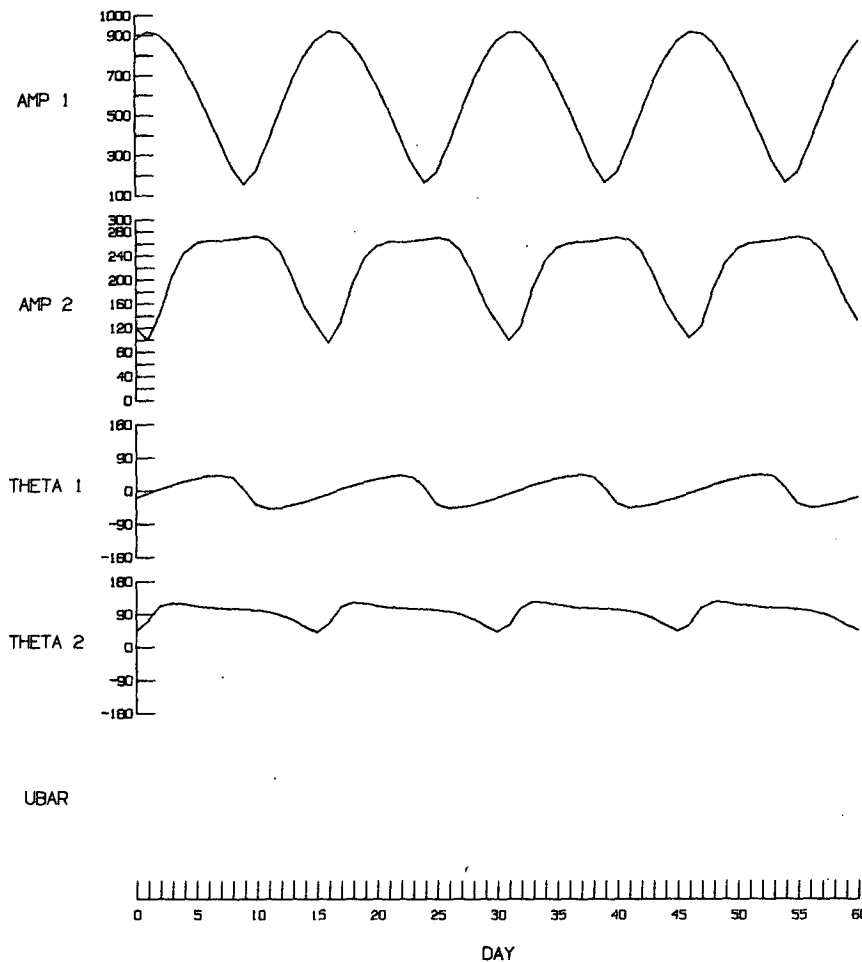


FIG. 19. As in Fig. 16 but for vacillation with fixed mean flow.

tween the stationary and traveling components of wave 1. Wave 2 vacillates because of temporal variations in its interaction with wave 1. Specifically, a rapid loss of wave 2 PE to wave 1 accompanies wave 1's gain of PE from the zonal flow during its increasing phase. Experiments with a barotropic model suggest that the interaction between the waves is governed by the interaction of wave 1 with the zonal flow, and that it is the wave 1-mean flow interaction that causes the decline of wave 2 to coincide with the amplification of wave 1. That wave-wave interactions should be catalyzed by wave-mean flow interactions is consistent with the results of Section 2. The interaction of a wave with the zonal flow implies that there is a component of the wave PV in quadrature with the wave's streamfunction. When wave-mean flow interactions are strong, this component of the wave PV is large, and this in turn leads to strong wave-wave interactions.

The model generates wave 1-wave 2 vacillations

which are realistic in several respects. The waves oscillate out of phase, variations in the mean flow are relatively weak, and the vacillations in the wave amplitudes are largely confined to the stratosphere. However the simple nature of the model raises questions about its applicability to the atmosphere. The rigid walls that bound the flow meridionally, the severe truncation, and the perfectly periodic westward traveling wave are its least realistic features. The first constraint means that the model can only treat interactions between waves confined within the natural channel created by the large meridional gradient of PV associated with the polar night jet. Wave-wave interactions at critical lines and wave breaking are excluded. The occurrence of the vacillation during periods when the zonal flow is relatively undisturbed suggests that the inclusion of the "surf zone" (McIntyre and Palmer, 1984), while obviously very important in the sudden warming, may not be essential in simulating the wave

1-wave 2 vacillation. The steadiness of westward wave 1 is clearly unrealistic in light of recent observations (Lindzen *et al.*, 1984). But there is strong support (Madden, 1983) for the idea that vacillations in the amplitudes of planetary waves and the strength of the mean flow result from interference between stationary and traveling waves. The results of Section 2 are sufficiently general that strong wave-mean flow interactions associated with this interference in the atmosphere would promote wave-wave interactions. The details of these interactions will presumably differ from those in a severely truncated model. So while the current model of the wave 1-wave 2 vacillation presents a plausible picture of how the vacillation could occur in the atmosphere, confirmation of these results will require detailed diagnoses of the vacillation both in observations and in the results of more comprehensive models.

*Acknowledgments.* This work was carried out by the author as a graduate student in the Department of Geological Sciences of Columbia University, working at the NASA Goddard Space Flight Center/Institute for Space Studies. He is grateful to the Institute for its support. Helpful comments were made by David Rind and Anthony Del Genio. Suggestions from Dr. Anne Smith and an anonymous reviewer have aided the author in improving the manuscript. The assistance of Harold Brooks with the word processor is appreciated.

#### REFERENCES

- Andrews, D. G., and M. E. McIntyre, 1976: Planetary waves in horizontal and vertical shear: the generalized Eliassen-Palm relation and the mean zonal acceleration. *J. Atmos. Sci.*, **33**, 2031-2047.
- Boyd, J. P., 1976: The noninteraction of waves with the zonally averaged flow on a spherical earth and the interrelationships of eddy fluxes of energy, heat and momentum. *J. Atmos. Sci.*, **33**, 2285-2291.
- Derome, J., 1984: On quasi-geostrophic, finite amplitude disturbances forced by topography and diabatic heating. *Tellus*, **36A**, 313-319.
- Dickinson, R. E., 1969: Theory of planetary wave-zonal flow interaction. *J. Atmos. Sci.*, **26**, 73-81.
- Geisler, J. E., 1974: A numerical model of the sudden stratospheric warming mechanism. *J. Geophys. Res.*, **79**, 4989-4999.
- Holton, J. R., and C. Mass, 1976: Stratospheric vacillation cycles. *J. Atmos. Sci.*, **33**, 2218-2225.
- , and W. M. Wehrbein, 1980: A numerical model of the zonal mean circulation of the middle atmosphere. *Pure Appl. Geophys.* **118**, 284-306.
- Labitzke, K., 1977: Interannual variability of the winter stratosphere in the Northern Hemisphere. *Mon. Wea. Rev.*, **105**, 762-770.
- Lindzen, R. S., B. Farrell and D. Jacqmin, 1982: Vacillations due to wave interference: Applications to the atmosphere and annulus experiments. *J. Atmos. Sci.*, **39**, 14-23.
- , D. M. Straus and B. Katz, 1984: An observational study of large-scale atmospheric Rossby waves during FGGE. *J. Atmos. Sci.*, **41**, 1320-1335.
- McIntyre, M. E., 1982: How well do we understand the dynamics of stratospheric warmings? *J. Meteor. Soc. Japan*, **60**, 37-65.
- , and T. N. Palmer, 1984: The "surf zone" in the stratosphere. *J. Atmos. Terr. Phys.*, **46**, 825-849.
- Madden, R. A., 1978: Further evidence of traveling planetary waves. *J. Atmos. Sci.*, **35**, 1605-1618.
- , 1983: The effect of the interference of traveling and stationary waves on time variations of the large-scale circulation. *J. Atmos. Sci.*, **40**, 1110-1125.
- Robinson, W. A., 1985: *Interactions among planetary waves and the generation of traveling long waves*. Ph.D. thesis, Columbia University, 268 pp.
- Simmons, A. J., 1974: Planetary-scale disturbances in the polar winter stratosphere. *Quart. J. Roy. Meteor. Soc.*, **100**, 76-108.
- Smith, A. K., 1983: Observation of wave-wave interactions in the stratosphere. *J. Atmos. Sci.*, **40**, 2484-2496.
- , J. C. Gille and L. V. Lyjak, 1984: Wave-wave interactions in the stratosphere: observations during quiet and active wintertime periods. *J. Atmos. Sci.*, **41**, 363-373.
- Tung, K. K., 1983: On the nonlinear versus linear lower boundary conditions for topographically forced stationary long waves. *Mon. Wea. Rev.*, **111**, 60-66.
- van Loon, H., *et al.*, 1973: Zonal harmonic standing waves. *J. Geophys. Res.*, **78**, 4463-4471.
- , R. A. Madden and R. L. Jenne, 1975: Oscillations in the Winter stratosphere. Part I: Description. *Mon. Wea. Rev.*, **103**, 154-162.
- Walterscheid, R. L., 1980: Traveling planetary waves in the stratosphere. *Pure Appl. Geophys.*, **118**, 239-265.